AIP | Applied Physics Letters

Opto-electric particle manipulation on a bismuth silicon oxide crystal

Michael Esseling, Stefan Glasener, Federico Volonteri, and Cornelia Denz

Citation: Appl. Phys. Lett. **100**, 161903 (2012); doi: 10.1063/1.4704361
View online: http://dx.doi.org/10.1063/1.4704361
View Table of Contents: http://apl.aip.org/resource/1/APPLAB/v100/i16
Published by the American Institute of Physics.

Opto-electric particle manipulation on a bismuth silicon oxide crystal

Michael Esseling,[a] Stefan Glasener, Federico Volonteri, and Cornelia Denz
Institute of Applied Physics, Westfälische-Wilhelms-Universität Münster, Corrensstrasse 2/4, 48149 Münster, Germany

(Received 10 December 2011; accepted 31 March 2012; published online 17 April 2012)

High-throughput manipulation of microparticles can be efficiently accomplished using electrokinetic effects. In this contribution, we demonstrate the two-dimensional investigation of internal space-charge fields inside a bismuth silicon oxide (BSO) crystal and their use for optically mediated particle trapping. The magnitude of the internal fields as well as the time constant for its build-up are measured by Zernike phase contrast and digital holography. The fast response time of a BSO crystal at very low light powers enables real-time generation of high electric field gradients. We demonstrate that this photoconductive material facilitates both electrophoretic and dielectrophoretic trapping of particles on an accessible surface. © *2012 American Institute of Physics*. [http://dx.doi.org/10.1063/1.4704361]

The highly attractive field of optical micromanipulation has brought up a number of innovative and sophisticated techniques to handle matter on the micro- and nanoscale. Optical tweezers (OTs), which were first discovered in the 1980s,[1] are no longer in their infancy and have matured to a powerful tool to enable a three-dimensional independent movement and orientation, e.g., to manipulate biological cells.[2,3] Much as they are suited for the precise handling of a few microparticles or bacteria, their expansion to large numbers of traps is often difficult due to a lack of sufficient laser power.

Different trapping techniques have been devised, though, which are capable of high-throughput particle manipulation, making use either of pressure gradients introduced by acoustic waves in fluid media[4] or the electric properties of matter and the resulting electrokinetic behaviour. Among the electrokinetic phenomena, the most important are electroosmotic forces changing the flow behaviour of a solvent,[5,6] electrophoretic forces that act on charged particles,[7,8] and dielectrophoretic (DEP) forces which are capable of manipulating uncharged matter[9–11] by interaction of a polarizable material with inhomogeneous electric fields. Although these systems are typically based on fixed, microfabricated electrodes,[12] new approaches using optical induction of so-called *virtual electrodes* on photoconductive materials have been proposed and demonstrated,[5,13] e.g., on the surface of a lithium niobate (LN) crystal.[14,15] These methods combine the capability for high capacity with the flexibility of optical tweezers. Additionally, in surface-based geometries, the active manipulation area remains accessible for easy integration into microfluidic devices.

In this letter, we present the use of a photorefractive bismuth silicon oxide (BSO) crystal for microparticle manipulation on its surface. Due to its significantly higher photoconductivity,[16] this material can overcome the major drawback for the use of lithium niobate—its long time constants—with the potential to generate forces in real-time. It has been shown that the internal electric fields originating from photorefractive crystals, such as LN, can be used to trap matter in air[14] as well as out of a microfluidic stream of particles.[15] We will show that the drift-induced internal electric fields in BSO, although significantly smaller than the photovoltaic fields in LN, are able to induce electrophoretic and dielectrophoretic forces. Since this material does not show considerable photovoltaic behaviour,[16,17] the application of an external electric field and the ensuing drift is the preferential way to induce highly modulated internal electric fields.[18] In order to measure the magnitude and structure of these fields, we utilize the linear electro-optic properties of BSO, which modify its refractive index by Pockels effect[18]

$$\Delta n = -\frac{1}{2} n_0^3 r_{\mathrm{eff}} E_{\mathrm{SC}}, \tag{1}$$

where Δn is the refractive index modulation, n_0 is the unmodified refractive index, r_{eff} is the effective component of the electro-optic tensor, and E_{SC} is the internal space-charge field. The refractive index modulation induces a relative phase shift $\Delta\varphi = \frac{\lambda}{2\pi} d\Delta n$ for a light wave of wavelength λ that is transmitted through a crystal of thickness d. Once the phase shifts are known, Eq. (1) allows the calculations of the internal electric fields. To measure the induced phase shifts, the (100) faces (Miller indices) of the (110) cut crystal are equipped with silver electrodes and the crystal is held between two copper spring contacts. A square-wave voltage with amplitude U_{peak} of up to 4 kV at different frequencies f is applied to the crystal. The front face is illuminated with a modulated, sinusoidal or binary, intensity pattern at a wavelength of 532 nm for the induction of a modulated internal electric field, whereas a 632.8 nm laser with a low power of 20 μW cm^{-1} is used for the two-dimensional holographic readout of the induced phase shift. Note that in our configuration, with the modulation grating vector $K \parallel [100]$, $r_{\mathrm{eff}} = r_{41} = 4.4\,\mathrm{pm\,V^{-1}}$ is assumed and optical activity is neglected.[16,19] The details of the off-axis digital holographic setup[20] as well as the numerical reconstruction of phase shifts by Fourier filtering and Hilbert transform are described elsewhere.[21]

[a]Electronic mail: michael.esseling@uni-muenster.de.

Several scientific contributions from the field of photorefractive optics report that in the case of a DC external voltage, screening charges at the electrical contact region distort and deteriorate the internal electric fields.[16,19] Additionally, in the case of an inhomogeneous illumination, the voltage drop across regions of high light intensity is less, effectively squeezing out the electric field from these regions. To avoid these effects, it has been proposed that an alternating field, whose period T is significantly shorter than the grating formation time, but longer than the free carrier lifetime, $\tau_g \gg T \gg \tau_{fcl}$, can be used to enhance the internal electric field.[22,23] Fig. 1 shows the measured magnitude of E_{SC} for the case of an applied DC voltage and square-wave voltage with a frequency of $f = 200$ Hz. The results clearly support the previous assumptions about the internal field, the modulation in the DC case is significantly lower than at 200 Hz, where the field is even enhanced above the value of the external field, $E_{int} = 260\ \mathrm{V\,mm^{-1}} > E_0 = 200\ \mathrm{V\,mm^{-1}}$. Another interesting fact is that if the external voltage is modulated in the suggested way,[22,23] the internal space-charge field becomes imaginary, resulting in a $\pi/2$ phase shift between incident light pattern and field modulation (see Fig. 1(b)). This effect has previously been used to facilitate amplitude-coupling in photorefractive two-wave-mixing experiments in BSO.[16,24] Deducing from the results in Fig. 1 and corresponding measurements for other frequencies, it can be concluded that for trapping with high fields and field gradients on BSO, external AC square-wave voltages with a frequency of $f > 100$ Hz should be used to avoid screening charges. It is important to note that this field enhancement is not a specific property of BSO or photorefractive materials in general, but is expected and may be exploited in materials that can be described following a similar model. The use of the electro-optic properties of BSO serves as a tool which facilitates the measurement of this behaviour.

A very important figure-of-merit in opto-electric trapping experiments is the response time of the material. Dielectrophoretic trapping experiments on a LN surface are drawn back by the long writing times for internal electric fields, which are on the order of minutes.[14,15] To determine the response time of BSO, an AC-biased crystal with the same geometry as before is integrated into a commercial Zernike phase-contrast microscope and illuminated with a binary stripe pattern. The refractive index modulation of this pattern can be directly visualized on a high-speed CCD camera without any numerical reconstruction. The light pattern is constantly switched on and off; the time-dependent visibility of the refractive index pattern is calculated from the camera grey values I as $V = (I_{max} - I_{min})/I_{mean}$. The switch-on and decay time constants can be approximated by a monoexponential fit with time constants $\tau_{decay} = 333$ ms and $\tau_{on} = 63$ ms (cf. Fig. 2). The longer decay times can be readily explained by the low dark conductivity of BSO, which is in orders of magnitude smaller than the conductivity in the illuminated state.[25] In particular, we measured for our sample $\sigma_{dark} = 1.14 \times 10^{-10}\ \mathrm{S\,cm^{-1}}$ and $\sigma_{photo} = 1.93 \times 10^{-6}\ \mathrm{S\,cm\,mW^{-1}}$. It can be concluded that a change of the electric field pattern, for which the illuminated state applies, can be accomplished in approximately 60 ms even at very low light powers of 3.5 mW $\mathrm{cm^{-1}}$. This value is in good agreement with time constants observed for BSO in other experiments, shorter response times could be achieved by increasing the illumination intensity.[16]

The previously described and analyzed internal electric fields present a tool for high-throughput manipulation of microparticles dispersed in a solvent. The resulting forces can be distinguished between electrophoretic and DEP forces[9]

$$F_{EP} = qE, \tag{2}$$

$$F_{DEP} = 2\pi r^3 \varepsilon_m K(\omega) \nabla E^2, \tag{3}$$

where q is the charge of the particle, E is the electric field, r is the particle radius, ε_m is the static dielectric permittivity of the solvent, $K(\omega)$ is the frequency-dependent complex Clausius-Mossotti factor, and ∇E^2 is the gradient of the squared electric field. While the electrophoretic force depends only on the particle charge, the DEP forces scales with the volume of particle as well as with the electric properties of dispersed matter and solvent, summarized in the Clausius-Mossotti factor. In the case of a low frequency electric field and spherical particles, it reduces to[26]

$$K(\omega \to 0) \approx \frac{\sigma_p - \sigma_m}{\sigma_p + 2\sigma_m}. \tag{4}$$

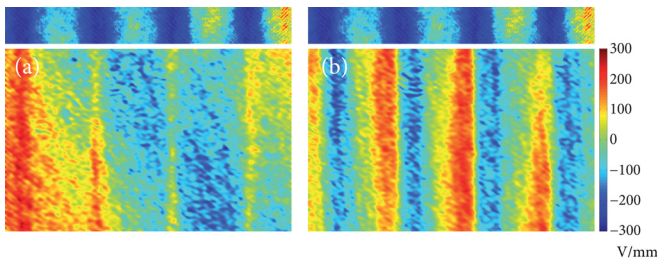

FIG. 1. Measurement of the internal electric field by digital holography: (a) in the case of a DC external voltage, the field modulation is lower and inhomogeneous, whereas with (b) an external square-wave voltage of $f = 200$ Hz, the internal field is significantly enhanced. Top row insets show the original sinusoidal intensity pattern that was incident on the crystal surface. Note the phase shift between the illumination pattern and the internal electric field for the AC case. The externally applied voltage was $U_{peak} = 3$ kV over a crystal length of $l_c = 15$ mm.

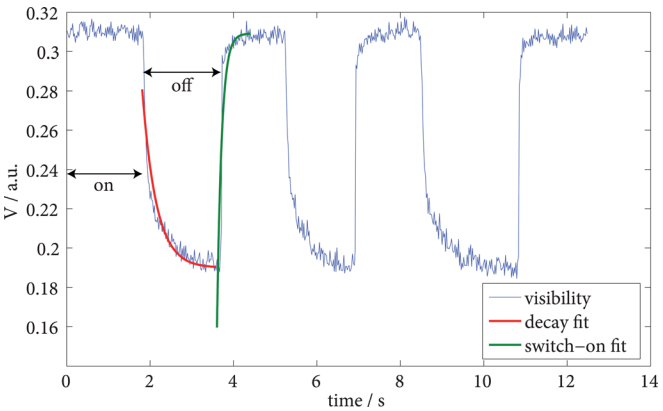

FIG. 2. Measurement of the build-up time constant for the internal electric field in BSO; a binary stripe pattern incident on the crystal is repeatedly turned on and off, while the visibility of the refractive index grating is visualized in Zernike phase contrast.

Hence, an attractive DEP force is exerted when the conductivity σ_p of the particle is higher than that of the surrounding medium (σ_m). To ensure this in our experiment, we use tetradecane (TD), an insulating alkane as the solvent. Test particles employed for DEP manipulation are uncharged graphite particles of sizes $6\,\mu m < d < 20\,\mu m$ suspended in TD. The AC-biased BSO crystal is integrated into a microscope, where it is illuminated from the bottom with a sinusoidal or binary stripe pattern while the alignment of matter is simultaneously observed from the top with infrared LED illumination. As observed in other experiments with lithium niobate,[14,15] particles align at the regions of high field gradients with a doubled spatial frequency, which results from the squared electric field in Eq. (3).

Fig. 3 further allows to correlate the particle positions with the original trapping pattern that is incident on the crystal. It is obvious that the regions of highest field gradients and hence highest DEP forces are $\pi/2$ phase-shifted compared to their expected position for the in-phase case. This phase shift is in very good agreement with the theory of grating formation with an alternating external field[23] and the results from the measurement of the internal electric field in Fig. 1. In the experiments concerning the DEP forces, we did not observe a dependence of the trapping strength on the frequency in the range that was tested, $100\,Hz \leq f \leq 500\,Hz$. However, with a frequency below 100 Hz, the trapping was significantly reduced and especially the frequency-doubled alignment of the test particles could not be observed, which can be attributed to the distorted field and the lower field gradients, as pointed out before.

In addition to the manipulation of neutral particles, electrostatic attraction of charged matter has also been observed. Ag-coated polystyrene (PS) microspheres ($d = 2\,\mu m$) are dispersed in TD which prevents discharge due to its insulating properties. Fig. 4 shows the PS beads being attracted to the dark regions of a square pattern that illuminates the AC-biased crystal. Assuming that electrons are the main charge carriers in BSO,[16] the dark regions can be associated with negative charge, indicating that the PS beads are positively charged.[27]

In conclusion, we have demonstrated electrokinetic particle manipulation on a bismuth silicon oxide crystal. The photorefractive properties offer a tool for direct access to the response time of the material as well as to the experimental conditions which give the best manipulation behaviour. Using our digital holographic measurement of the phase retardations inside BSO, we could directly verify that the internal electric field is indeed $\pi/2$ phase-shifted with respect to the original light modulation and that its magnitude can be enhanced above the value of its external counterpart, a beneficial effect that is not limited to bismuth silicon oxide and can be exploited also in other materials.[28] The use of BSO for electrokinetic trapping benefits from the crystal's high durability against many solvents and its relatively fast response time that enables a real-time generation of virtual electrodes at low light power. Due to the planar geometry with side-equipped electrodes, the active surface remains accessible for easy integration into microfluidic components. It has been demonstrated that the internal electric fields, although significantly smaller than in lithium niobate, can be utilized for electrophoretic as well as dielectrophoretic trapping. The trapping efficiency, which is at the moment limited by the moderate external voltage drops over a long crystal, can be significantly improved by decreasing the size of the active manipulation area. Further work towards such an improvement is currently being pursued. Additionally, the application of an external voltage yields an additional degree of freedom as compared to the previous experiments on lithium niobate,[15] since it is now possible to instantly tune frequency, magnitude, and—with the application of perpendicular electrodes—direction of the electric field.

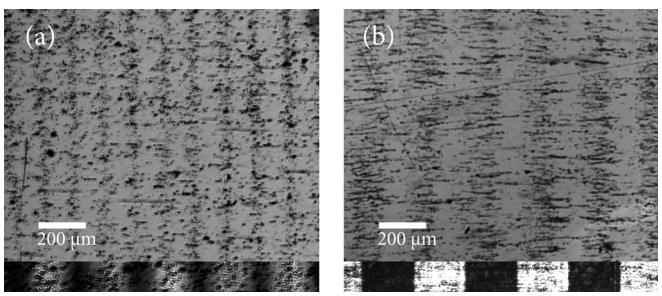

FIG. 3. Dielectrophoretic trapping of graphite test particle on an AC-biased BSO surface ($l_c = 10\,mm$, $f = 100\,Hz$, $U_{peak} = 3.3\,kV$; the crystal was illuminated with (a) a sinusoidal interference pattern with a period of $\Lambda = 257\,\mu m$ and (b) a binary stripe pattern with a period of $\Lambda = 430\,\mu m$, respectively. In both cases, test particles align with a doubled spatial frequency; bottom insets show original light pattern incident upon the crystal; the electric field direction is from left to right.

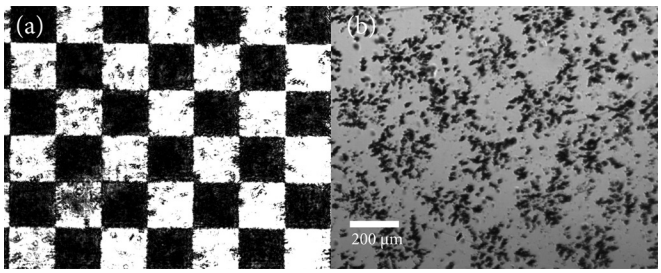

FIG. 4. Electrophoretic trapping of positively charged polystyrene microbeads. (a) Square wave pattern incident on the BSO crystal. (b) Microbeads trapped in regions of negative charge; parameters for the applied voltage are the same as in Fig. 3.

This work was financially supported by DFG Grant TRR61 and the European Commission in the frame of Photonics4Life (P4L).

[1]A. Ashkin, J. Dziedzic, and T. Yamane, Nature (London) **330**, 769 (1987).
[2]D. G. Grier, Nature (London) **424**, 810 (2003).
[3]F. Hoerner, M. Woerdemann, S. Mueller, B. Maier, and C. Denz, J. Biophotonics **3**, 468 (2010).
[4]J. Shi, D. Ahmed, X. Mao, S.-C. S. Lin, A. Lawit, and T. J. Huang, Lab Chip **9**, 2890 (2009).
[5]R. Hayward, D. Saville, and I. Aksay, Nature (London) **404**, 56 (2000).
[6]T. Gong and D. Marr, Appl. Phys. Lett. **85**, 3760 (2004).
[7]C. Cabrera and P. Yager, Electrophoresis **22**, 355 (2001).
[8]X. Xuan and D. Li, Electrophoresis **26**, 3552 (2005).
[9]H. Pohl, J. Appl. Phys. **29**, 1182 (1958).
[10]H. Morgan, N. Green, M. Hughes, W. Monaghan, and T. Tan, J. Micromech. Microeng. **7**, 65 (1997).
[11]K. Kang, X. Xuan, Y. Kang, and D. Li, J. Appl. Phys. **99**, 064702 (2006).
[12]C. Zhang, K. Khoshmanesh, A. Mitchell, and K. Kalantar-zadeh, Anal. Bioanal. Chem. **396**, 401 (2010).
[13]P. Chiou, A. Ohta, and M. Wu, Nature (London) **436**, 370 (2005).

[14]H. A. Eggert, F. Y. Kuhnert, K. Buse, J. R. Adleman, and D. Psaltis, Appl. Phys. Lett. **90**, 241909 (2007).
[15]M. Esseling, F. Holtmann, M. Woerdemann, and C. Denz, Opt. Express **18**, 17404 (2010).
[16]M. Petrov and V. Bryksin, "Space-charge waves in sillenites: Rectification and second-harmonic generation" in *Photorefractive Materials and Their Applications 2: Materials* (Springer, 2007), pp. 285–325.
[17]B. Sturman and V. Fridkin, *The Photovoltaic and Photorefractive Effects in Noncentrosymmetric Materials* (Gordon and Breach, 1992).
[18]P. Yeh, *Introduction to Photorefractive Nonlinear Optics* (Wiley Interscience, 1993).
[19]A. Grunnet-Jepsen, I. Aubrecht, and L. Solymar, J. Opt. Soc. Am. B **12**, 921 (1995).
[20]B. Kemper and G. von Bally, Appl. Opt. **47**, A52 (2008).
[21]T. Ikeda, G. Popescu, R. Dasari, and M. Feld, Opt. Lett. **30**, 1165 (2005).
[22]A. Grunnet-Jepsen, C. Kwak, I. Richter, and L. Solymar, J. Opt. Soc. Am. B **11**, 124 (1994).
[23]S. Stepanov and M. Petrov, Opt. Commun. **53**, 292 (1985).
[24]G. Pauliat, C. Besson, and G. Roosen, IEEE J. Quantum Electron. **25**, 1736 (1989).
[25]A. Attard, Appl. Opt. **28**, 5169 (1989).
[26]T. Jones, *Electromechanics of Particles* (Cambridge University Press, 1995).
[27]X. Zhang, J. Wang, B. Tang, X. Tan, R. A. Rupp, L. Pan, Y. Kong, Q. Sun, and J. Xu, Opt. Express **17**, 9981 (2009).
[28]J. Kumar, G. Albanese, W. Steuer, and M. Ziari, Opt. Lett. **12**, 120 (1987).